

Synthesis, Photophysics, and Electroluminescence of Copolyfluorenes Containing Jacketed and Silyl Units

Ping Wang, Qian Yang, Hao Jin, Wanli Liu, Zhihao Shen, Xiaofang Chen, Xinghe Fan,*
Dechun Zou,* and Qifeng Zhou*

Beijing National Laboratory for Molecular Sciences, Key Laboratory of Polymer Chemistry and Physics
of Ministry of Education, College of Chemistry and Molecular Engineering, Peking University,
Beijing 100871, People's Republic of China

Received July 18, 2008; Revised Manuscript Received September 4, 2008

ABSTRACT: New copolyfluorenes (**PSiC8OF0**~**PSiC8OF50**) composed of 9,9-dioctylfluorene, jacketed units 2,5-bis[(5-octyloxy-phenyl)-1,3,4-oxadiazole]-1-(3,5-dibromophenyl)-benzene (**35C8**) and 2,5-bis(trimethylsilyl)benzene were synthesized by palladium-catalyzed Suzuki coupling reaction. They were characterized by GPC, ¹H NMR, elemental analysis, DSC, TGA, absorption and emission spectroscopy, and cyclic voltammetry (CV). These copolymers were readily soluble in common organic solvents and exhibited high glass transition temperature (up to 173 °C). The copolymer films showed absorption peaks from 325 to 337 nm, and PL peaks from 402 to 408 nm with a great blue shift relative to polyfluorene (377 and 432 nm) originated from silyl and jacketed units. The transient PL spectra show a rapid rise in the lifetime, implying a sharp increase in molecular rigidity and an additional long decay time around 5~6 ns, assigned to an “excimer-like” state, and its contribution increases with the increased jacketed fraction. The HOMO energy levels and LUMO levels changed from –5.59~–6.07 eV and –2.60~–3.01 eV as the incorporation of silyl and jacketed units, which facilitated electron injection. Electroluminescent devices: ITO/PEDOT:PSS/PVK/polymer/TPBI (15nm)/Ca (30 nm)/Ag (80 nm) were fabricated to investigate the influence of jacketed and silyl contents on the emission characteristics. The maximum current efficiency and external quantum efficiency of the **PSiC8OF5** device (0.484 cd/A and 1.35%) surpassed those of the **PC8OF0** device (0.416 cd/A and 0.51%). The EL emissions of **PSiC8OF0** and **PSiC8OF5** were bright blue and pure blue with sharp emissions, respectively, while **PSiC8OF10**~**PSiC8OF50** showed emissions between them. This indicates that copolymer **PSiC8OF5** could be a good candidate for blue light-emitting materials.

Introduction

Conjugated polymers and copolymers are drawing wide interest for applications in large-area flexible and tunable polymeric light-emitting diodes (PLEDs).^{1–5} Among the three primary colors, the pursuit of blue light-emitting materials with high efficiency and good color purity still remains as a challenge. Poly(fluorene)s (PFs) with large band gaps have been widely studied as promising materials for blue emission due to their unique combination of high thermal stability, high hole mobility, easy processability, and high photoluminescence (PL) quantum yield in the solid state.⁶ However, the major drawback of PFs is that they display a red-shifted and diminished emission upon thermal annealing or passage of current. The source of this long wavelength emission was attributed to excimer emission and keto defects of the polymer backbone.⁷ Numerous strategies have been adopted to suppress this red-shifted and less efficient emission.⁸ However, the long wavelength emission was still under study and further internal mechanisms were still needed. Blue-emitting PF is a p-type (electron donor, hole transport) material that transports holes with high mobility,⁹ and electron injection and transport in PF is relatively poor. Oxadiazoles are among the first and most extensively investigated class of electron-transporting materials.¹⁰ Oxadiazole (OXD) moieties have been widely employed as an electron-transporting unit in the study of polymer LEDs.¹¹

Recently, there has been increasing interest in the silyl-substituted luminescent polymers, in which silyl moieties are introduced either as side chains or as a segment integrated into the polymer backbones.¹² It has been reported that bis-silyl

substitution affords the PPV further improved amorphousness and sharp emission because of the larger atomic size of Si and the longer bond length of C–Si.¹³ It was reported that the trimethylsilyl substituent was nonelectron-donating and will facilitate for electron injection.¹⁴ Therefore, it is meaningful to design and synthesize bis-silyl substituted copolymers with the aim of improving the processability and carrier balance.

According to the theory of mesogen-jacketed liquid crystalline polymers:¹⁵ when side chains are attached laterally to the gravity centers of the main chain without spacers, the main chain of polymers are forced to extend and to conform rigidly because of high population of both bulky and rigid side groups around the backbone and the “jacket” is formed. Our motivation for the present work was to synthesize copolymers composed of bis-silyl and jacketed moieties with electron-deficient (n-type) side-chain building block to improve the flexibility and carrier balance to improve the electroluminescent efficiencies.

In this contribution, we present the synthesis of alternating copolymers of 9,9-dioctylfluorene with jacketed derivatives (**35C8**) and bis-silyl groups through the Suzuki coupling reaction. The general properties of these copolymers, including thermal, optical, and electrochemical properties, are discussed. Furthermore, the potential application of these copolymers as active layers in PLEDs is systematically investigated.

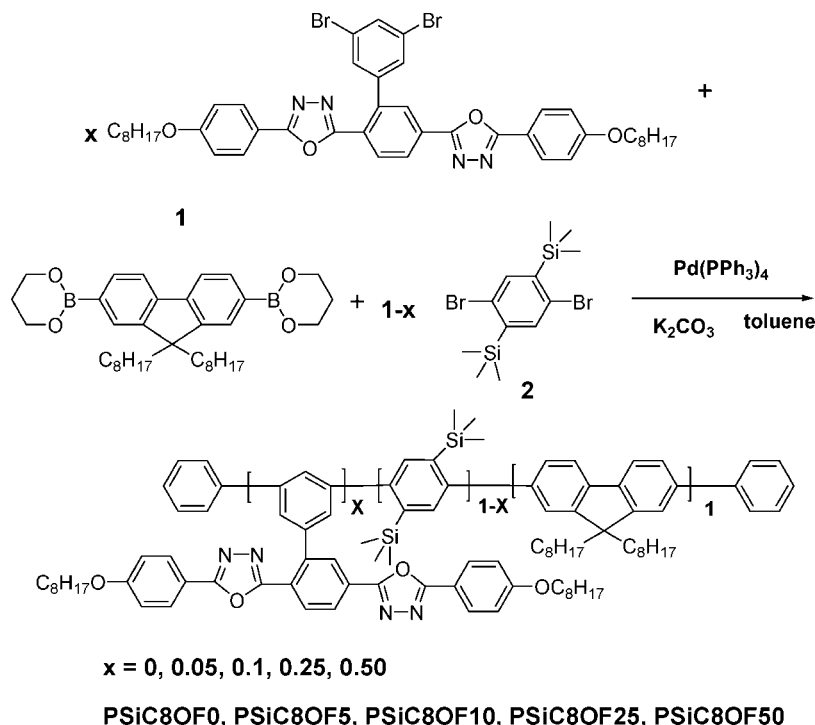
Experimental Details

Materials. 9,9-dihexyl-2,7-dibromofluorene was obtained from Synwit Technology Co., Ltd. 9,9-dioctylfluorene-2,7-bis(trimethylsilyl)fluorene and Chlorotrimethylsilane was purchased from Aldrich and used as received.

Measurements. ¹H NMR spectra were recorded on a Mercury plus 300 MHz or Bruker 400 MHz using CDCl₃ as solvent in all cases. Elemental analyses were carried out on Elementar Vario EL (Germany). Gel permeation chromatographic (GPC) measurements

* To whom correspondence should be addressed. E-mail: Xinghe Fan (fanxh@pku.edu.cn); Dechun Zou (dczou@pku.edu.cn); and Qifeng Zhou (qfzhou@pku.edu.cn).

Scheme 1. Synthetic Routes of the Copolymers



were carried out at 35 °C on a Waters 2410 instrument equipped with three Waters μ -Styragel columns (10^3 , 10^4 , and 10^5 Å) in series, using THF as the eluent at a flow rate of 1.0 mL/min. All of the GPC data were calibrated with polystyrene standards. The thermogravimetric analysis (TGA) was performed with a Q600 SDT instrument at a heating rate of 20 °C/min in nitrogen atmosphere.

Differential scanning calorimetry (DSC, PerkinElmer Pyris 1 with a mechanical refrigerator) was utilized to study the glass transitions of the polymers. A typical DSC sample size was ~5 mg. The samples were encapsulated in hermetically sealed aluminum pans, and the pan weights were kept constant. The temperature and heat flow scale at different cooling and heating rates were calibrated using standard materials such as indium and benzoic acid. The glass transition temperatures (T_g) were obtained from the second heating curve.

Absorption spectra were measured with a Jasco V-550 spectrophotometer, and PL spectra were obtained using a Hitachi F-4500 fluorescence spectrophotometer.

The time-resolved fluorescence measurements were performed using the time-correlated single-photon counting technique following excitation by a nanosecond flash lamp (Edinburgh Instruments FL900).

The cyclic voltammograms were recorded using a voltammetric analyzer (CHI630C from Shanghai Chenhua Instrument Company, China) at room temperature under nitrogen atmosphere. The measuring cell consisted of polymer-coated Pt as the working electrode, Ag/AgCl electrode as reference electrode, and platinum wire electrode as auxiliary electrode, supporting in 0.1 M (*n*-Bu)₄NClO₄ in acetonitrile. Prior to each series of measurements, the cell was deoxygenated with argon. The energy levels were calculated using the ferrocene (FOC) value of -4.8 eV with respect to vacuum level, which is defined as zero.¹⁶ Two drops of ferrocene (1 M in acetonitrile) were added and the measured oxidation potential of ferrocene (E_{FOC}) (vs Ag/AgCl) was $\text{FOC} = (0.50 + 0.60)/2 = 0.55$ eV. Therefore, the HOMO level of the polymers could be calculated by the equation $E_{\text{HOMO}} = -[E_{\text{onset(ox)}} + (4.8 - 0.55)]$ eV and the LUMO level could be estimated by the equation $E_{\text{LUMO}} = -[E_{\text{onset(red)}} + (4.8 - 0.55)]$ eV.

Device Fabrication and Characterization. The fabrication process of the diodes followed a standard procedure below. The patterned ITO (indium tin oxide) substrate was cleaned with

Table 1. Molecular Weights and Thermal Properties of the Copolymers

polymers	M_n^a	PDI ^a	T_g (°C) ^b	T_d (°C) ^c
PSiC8OF0	13000	2.05	118	424
PSiC8OF5	15400	2.12	125	418
PSiC8OF10	10900	2.71	173	416
PSiC8OF25	9400	2.47	165	404
PSiC8OF50	10100	3.41	145	397

^a M_n and PDI of the polymers were determined by GPC using polystyrene standards. ^b Evaluated by DSC during second heating cycle at a rate of 10 °C/min. ^c The temperature at which 5% weight loss of the sample was reached from TGA under nitrogen atmosphere.

detergents and deionized water, and finally treated with UV-ozone for about 25 min. PEDOT (purchased from Bayer) was spin coated on the preclean ITO substrate and dried by baking in air at 120 °C for 10 h. PVK was spin coated from 1,1,2,2-tetrachloroethane solution (10 mg/mL) and dried by baking in air at 150 °C for 2 h. Then, the copolymer was spin-casted from toluene solution (10 mg/mL) through a 0.45 μm Teflon filter. The thickness of the spin-coated film was controlled by regulating the spinning speed. Then the coated ITO was transferred into a deposition chamber with a base pressure of 1×10^{-6} Torr, TPBI and Metal layer was evaporated onto the polymer layer. The emitting area was 2×2 mm. The EL spectra were measured with a spectrofluorometer FP-6200 (JASCO). A source-measure unit R6145 (Advantest), multimeter 2000 (Keithley) and luminance meter LS-110 (Minolta) were used for I-V-L measurements. Relative luminance was directly detected by using a multifunctional optical meter 1835-C (Newport).

Synthesis of Monomers (Scheme 1) 2,5-Bis[(5-octyloxy-phenyl)-1,3,4-oxadiazole]-1-(3,5-dibromophenyl)-benzene (1) (35C8). 2,5-Bis[(5-octyloxy-phenyl)-1,3,4-oxadiazole]-1-(3,5-dibromophenyl)-benzene was synthesized according to previous reports.¹⁷ ¹HNMR (CDCl₃, 300 MHz, ppm): 8.42–8.45 (1H, d, Ar-H), 8.30–8.33 (1H, d, Ar-H), 8.07–8.16 (3H, q, Ar-H), 7.80–7.81 (1H, t, Ar-H), 7.68–7.71 (2H, d, Ar-H), 7.54–7.55 (2H, d, Ar-H), 7.02–7.05 (2H, d, Ar-H), 6.95–6.98 (2H, d, Ar-H), 4.00–4.07 (4H, q, -OCH₂), 1.80–1.85 (4H, m, CH₂), 1.30–1.49 (20H, m, CH₂), 0.87–0.92 (6H, t, CH₃). Anal. Calcd. For C₄₄H₄₈Br₂N₄O₄: C, 61.69; H, 5.65; N, 6.54. Anal. Found: C, 62.07; H, 5.79; N, 6.51.

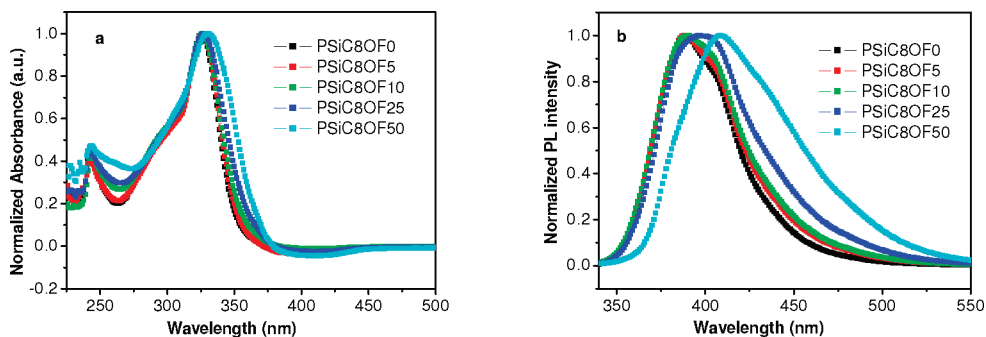


Figure 1. (a) Normalized absorption and (b) Normalized PL spectra (excitation: 326 nm) of copolymers in chloroform (1×10^{-6} M).

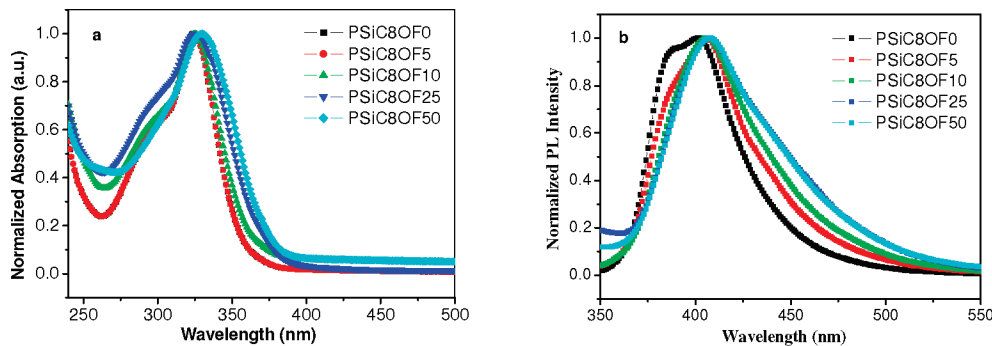


Figure 2. (a) Normalized absorption and (b) Normalized PL spectra of copolymers in the film state.

Table 2. UV-Vis and PL Data in CHCl_3 Solution and in Films

polymers	UV (sol/nm) ^a	UV (film/nm)	PL(sol/ nm) ^a	PL(film/ nm)
PSiC8OF0	326	325	388	402
PSiC8OF5	326	325	388	406
PSiC8OF10	326	326	390	405
PSiC8OF25	327	326	399	408
PSiC8OF50	330	330	409	408

^a In chloroform (1×10^{-6} M).

1,4-Dibromo-2,5-bis(trimethylsilyl)benzene (2). 1,4-Dibromo-2,5-bis(trimethylsilyl)benzene was synthesized according to previous references.¹⁸ ^1H NMR (CDCl_3 , 300 MHz, ppm): 7.51 (s, 2H), 0.38 (s, 18H). Anal. Calcd for $\text{C}_{12}\text{H}_{20}\text{Br}_2\text{Si}_2$: C, 37.90; H, 5.30. Found: C, 37.92; H, 5.17.

General Polymerization Procedure. Under an argon atmosphere, 9,9-dioctylfluorene-2,7-bis(trimethyleneborate), 2,5-bis[(5-octyloxy-phenyl)-1,3,4-oxadiazole]-1-(3,5-dibromophenyl)-benzene (**1**), 1,4-Dibromo-2,5-bis(trimethylsilyl)benzene (**2**) were mixed together with 2 mol % of $\text{Pd}(\text{PPh}_3)_4$, degassed toluene, and 2 M aqueous potassium carbonate solution. The mixture was degassed and vigorously stirred at $80\sim 90^\circ\text{C}$ for 72 h. At the end of polymerization, small amounts of phenylboronic acid were added to remove bromine end groups, and bromobenzene was added as a monofunctional end-capping reagent to remove boronic acid end group. Then the mixture was extracted with dichloromethane and water, and the combined organic extracts were concentrated and were poured into stirred 200 mL of methanol to precipitate a plenty of solids. The solid was collected by filtration and washed with methanol. The polymer was further purified by washing with refluxing acetone in Soxhlet for 3 days and was dried under vacuum to afford the desired polymers. The resulting materials were soluble in THF, chloroform, and toluene.

PSiC8OF0. ^1H NMR (CDCl_3 , 300 MHz, ppm): 7.82–7.84 (2H, d, Ar–H), 7.60 (2H, m, Ar–H), 7.43 (4H, m, Ar–H), 2.04 (4H, br, $-\text{CH}_2$), 1.12–0.80 (30H, m, CH_2 and CH_3), 0.07–0.12 (18H, br, $-\text{CH}_3$). Anal. Found: C, 79.02; H, 9.59.

PSiC8OF5. ^1H NMR (CDCl_3 , 300 MHz, ppm): 8.47 (0.42H, m, Ar–H), 8.36 (0.42H, m, Ar–H), 8.14 (0.41H, m, Ar–H), 7.82–7.84 (2H, d, Ar–H), 7.60 (2H, m, Ar–H), 7.43 (4H, m, Ar–H), 7.06 (0.20H, d, Ar–H), 6.81 (0.22H, d, Ar–H), 4.05

Table 3. Fluorescence Decay Lifetimes of the Copolymers in CHCl_3 Solutions under Excitation Using Absorption λ_{max}

polymers	detecting wavelength (nm)	τ (ns)	χ^2	rel %
PC8OF0 ^a	415	0.47	1.064	100
PSiC8OF0	388	0.58	0.855	100
PSiC8OF5	388	0.74	0.868	93.62
		6.29		6.38
PSiC8OF10	390	0.53	0.914	92.53
		5.53		7.47
PSiC8OF25	399	0.68	1.116	73.90
		5.42		26.10
PSiC8OF50	409	0.42	0.999	23.14
		2.54		40.80
		6.23		36.05

^a Ref 17.

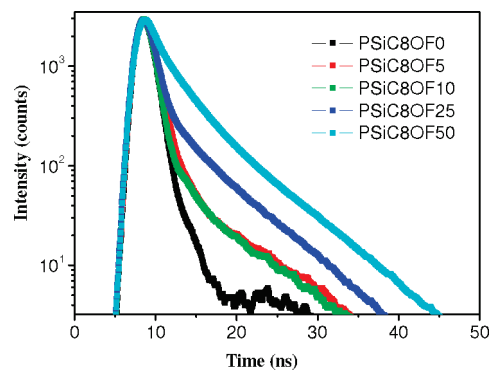


Figure 3. Fluorescence decay curves of PSiC8OFs in dilute CHCl_3 solutions (10^{-6} M).

(0.21H, m, $-\text{OCH}_2$), 3.91 (0.25H, m, $-\text{OCH}_2$), 2.04 (4H, br, $-\text{CH}_2$), 1.12–0.80 (30H, m, CH_2 and CH_3), 0.07–0.12 (18H, br, $-\text{CH}_3$). Anal. Found: C, 78.57; H, 9.31.

PSiC8OF10. ^1H NMR (CDCl_3 , 300 MHz, ppm): 8.46 (0.42H, m, Ar–H), 8.36 (0.42H, m, Ar–H), 8.14 (0.41H, m, Ar–H), 7.84 (2.13H, m, Ar–H), 7.60 (2.16H, m, Ar–H), 7.43 (3.15H, m, Ar–H), 7.06 (0.35H, d, Ar–H), 6.81 (0.21H, d, Ar–H), 4.05 (0.35H, m, $-\text{OCH}_2$), 3.91 (0.38H, m, $-\text{OCH}_2$), 2.04 (4H, br, $-\text{CH}_2$),

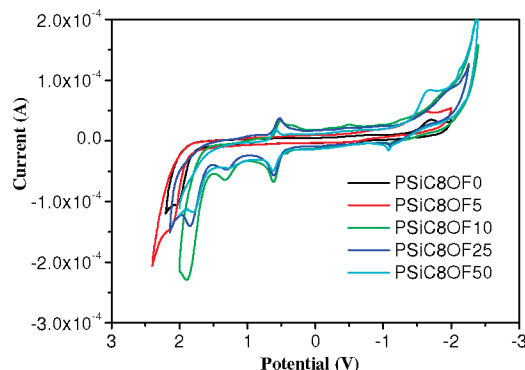


Figure 4. Cyclic voltammograms of copolymer films coated on Pt electrode (scan rate: 100 mV/s).

Table 4. Electrochemical Properties of the Copolymers

	red _{onset} ^a V	Ox _{onset} ^b V	HOMO (eV)	LUMO (eV)	E _g (eV) ^c
PC8OF0 ^d		1.24	-5.59	-2.60	2.99 ^d
PSiC8OF0	-1.41	1.78	-6.03	-2.84	3.19
PSiC8OF 5	-1.24	1.82	-6.07	-3.01	3.06
PSiC8OF 10	-1.46	1.62	-5.87	-2.79	3.08
PSiC8OF 25	-1.38	1.61	-5.86	-2.87	2.99
PSiC8OF 50	-1.41	1.59	-5.84	-2.84	3.00

^a Onset reduction potential measured by cyclic voltammetry. ^b Onset oxidation potential measured by cyclic voltammetry. ^c E_g stands for energy band gap estimated from E_g = HOMO–LUMO.^d Ref 17 and the E_g estimated from the UV–vis absorption edges in the film-state.

1.12–0.80 (30H, m, CH₂ and CH₃), 0.07–0.12 (18H, br, –CH₃) Anal. Found: C, 72.31; H, 8.07; N, 0.62.

PSiC8OF25. ¹H NMR (CDCl₃, 300 MHz, ppm): 8.46 (0.81H, m, Ar–H), 8.36 (0.72H, m, Ar–H), 8.14 (0.74H, m, Ar–H), 7.85 (2.2H, m, Ar–H), 7.71 (1.1H, m, Ar–H), 7.63 (2.46H, m, Ar–H), 7.43 (3.16H, m, Ar–H), 7.06 (0.54H, d, Ar–H), 6.81 (0.64H, d, Ar–H), 4.05 (0.62H, m, –OCH₂), 3.91 (0.74H, m, –OCH₂), 2.04 (4H, br, –CH₂), 1.12–0.80 (30H, m, CH₂ and CH₃), 0.07–0.12 (18H, br, –CH₃) Anal. Found: C, 77.14; H, 8.50; N, 1.39.

PSiC8OF50. ¹H NMR (CDCl₃, 300 MHz, ppm): 8.46 (1.2H, m, Ar–H), 8.36 (1.1H, m, Ar–H), 8.14 (1.3H, m, Ar–H), 7.85 (2.2H, m, Ar–H), 7.71 (2.2H, m, Ar–H), 7.63 (3H, m, Ar–H), 7.43 (2H, m, Ar–H), 7.06 (1.2H, d, Ar–H), 6.81 (1.3H, d, Ar–H), 4.05 (1.2H, m, –OCH₂), 3.91 (1.2H, m, –OCH₂), 2.04 (4H, br, –CH₂), 1.12–0.80 (30H, m, CH₂ and CH₃), 0.07–0.12 (18H, br, –CH₃) Anal. Found: C, 78.12; H, 7.96; N, 3.23.

Results and Discussion

Synthesis and Characterization. The well-defined fluorene-containing copolymers were synthesized by the Suzuki cross-coupling reaction. The synthetic route is illustrated in Scheme 1. All of these copolymers were readily soluble in common organic solvents such as chloroform, THF, chlorobenzene, and toluene. And their molecular structures were verified by ¹H NMR spectroscopy, elemental analysis. The incorporation of the monomer (**1**) and monomer (**2**) unit into the copolymer backbone was indicated by the observation of their characteristic signals and their clear assignments in the NMR spectra. For example, peaks at around 4.05 and 3.92 ppm in ¹H NMR spectra were assigned to the alkoxy protons in the side chain of **1**; peaks at around 0.06–0.11 ppm were assigned to the trimethylsilyl protons in the side chain of **2**. The number-average molecular weights (*M_n*) of the copolymers, obtained by gel permeation chromatography (GPC) using THF as the eluent and polystyrene as standards, ranged between 9400 and 13 000 with a polydispersity index of 2.05–3.41.

Thermal Analysis. The thermal properties of the copolymers were evaluated by thermogravimetric analysis (TGA) and differential scanning calorimetry (DSC) under a nitrogen atmosphere. The results are presented in Table 1. All materials exhibited an onset of decomposition around 400 °C with no weight loss at lower temperature, suggesting their outstanding thermal stability. The glass transition temperatures (*T_g*) of copolymers were improved from 118 to 173 °C. Copolymers **PSiC8OF0** showed glass transitions at around 118 °C. As the content of jacketed units increased, **PSiC8OF10** had the highest glass transition at 173 °C. When the content of jacketed units increased further, the glass transition decreased a little to 145 °C for **PSiC8OF50**. The results suggested that both the content of rigid jacketed moiety (**1**) and 2,5-bis(trimethylsilyl)benzene (**2**) effectively improved the *T_g* of polymers.

Photophysical Properties. The normalized absorption and PL emission spectra of copolymers in dilute CHCl₃ solutions (10^{−6} M) and in films are shown in Figures 1~2 and the corresponding spectra data are shown in Table 2. **PSiC8OF0** in CHCl₃ solution exhibits absorption with a λ_{max} at 326 nm, which is far more blue-shifted compared to polyfluorene absorption (377 nm). This is originating from the lack of electron donating ability and sterical hindrance of the trimethylsilyl substituent.¹⁹ Moreover, the absorption spectra exhibit a gradual red-shift with an increase in **35C8** fractions, that is, from 326 nm in **PSiC8OF0** to 330 nm in **PSiC8OF50**. This effect also manifests itself in the solution PL spectra, where the emission peaks are red-shifted from 388 nm in **PSiC8OF0** to 409 nm in **PSiC8OF50**. Figure 1(b) shows the PL spectra of copolymers in CHCl₃ solutions. This may be attributed to the large π-conjugated side chains of **35C8**. In comparison to dilute solutions, the absorption and emission spectra of films spin-coated on quartz substrates show slightly bathochromic shift, and some broadening of the absorption bands in comparison with their solution absorption spectra. It can be seen in Figure 2 that as the **35C8** fractions increased to **PSiC8OF50**, the maximum emission shows no red-shift compared to that in solutions, which maybe attributed to the big sterical hindrance of the jacketed structures.

Time-Resolved Photoluminescence Decay Dynamics. To develop a better understanding of the fluorescence behavior of **PSiC8OFs**, the fluorescence decay was measured by using a time-correlated single-photon counting technique. Fluorescence decay curves were analyzed using the least-squares interactive convolution method. The fluorescence decay parameters in solutions are collected in Table 3, and Figure 3 showed the fluorescence decay curves of the blue emission peaks in dilute CHCl₃ solutions for elucidation. All materials were excited with the maximum absorption wavelengths and detected with the maximum emission wavelengths. The transients can be fitted by a monoexponential function for **PSiC8OF0** and multiexponential function for **PSiC8OF5~PSiC8OF50**. The quality of the fits has been judged by the fitting parameters χ² < 1.2. The fluorescence intensity of **PSiC8OF0** decays single exponentially with a decay time of 0.58 ns. However, as the jacketed segment increases in the copolymer, the contribution of an additional long decay component of 6.29~5.42 ns is found and increases. This emission could be assigned to an excited-state excimer-like chromophore–chromophore interaction.²⁰ Moreover, a rapid rise in the lifetime was found from **PSiC8OF0** to **PSiC8OF50** as shown in Figure 3, implying a sharp increase in molecular rigidity.²¹

Electrochemical Properties. Cyclic voltammogram (CV) is a useful method for measuring electrochemical behaviors and evaluation of the relative HOMO, LUMO energy levels and the band gap of a polymer. Cyclic voltammetry (CV) of the

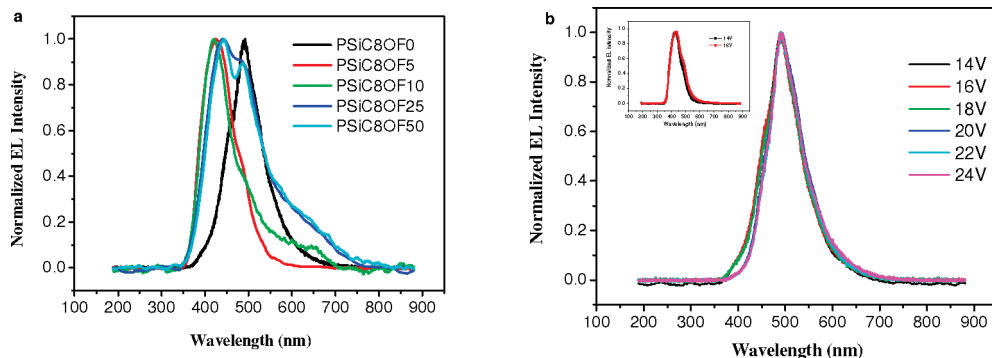


Figure 5. (a) EL spectra of copolymers at low voltages under device a. (b) EL spectra of **PSiC8OF0** under different voltages, inset were the EL Spectra of **PSiC8OF5** under different voltages.

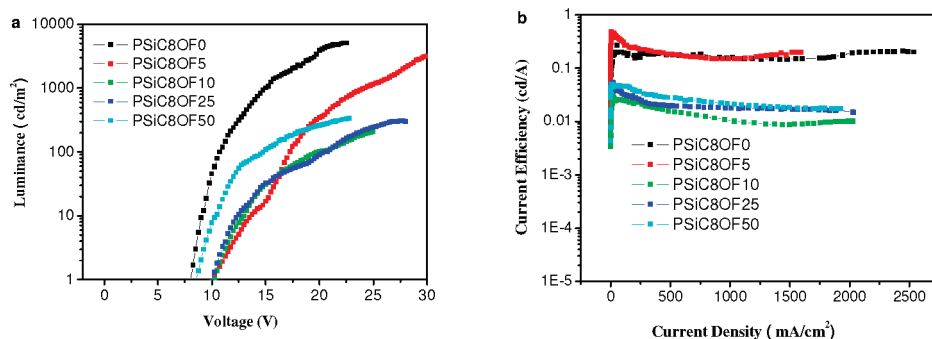


Figure 6. (a) Luminance-voltage characteristics and (b) Current efficiency-current density characteristics of copolymers with the configuration of device b.

Table 5. Electroluminescent Performances under Device b: ITO/PEDOT/PVK /Polymer/TPBI/Ca/Ag

polymers	U_{onset} /V	L_{max} /cdm ⁻²	η_{imax} /cdA ⁻¹	CIE coordinate	η_{extmax} %	λ/nm (low voltage)
PC8OF0 ^a	4.5	3122.8	0.416	0.16,0.07	0.514	426,449
PSiC8OF0	8.1	5105.4	0.267	0.18,0.31	0.143	491
PSiC8OF5	10.2	3163.0	0.484	0.14,0.05	1.350	426
PSiC8OF10	10.2	203.6	0.0257	0.19,0.14	0.031	426(484)
PSiC8OF25	10.1	308.2	0.0545	0.21,0.21	0.034	440,488
PSiC8OF50	8.6	337.6	0.0499	0.22,0.22	0.032	440,491

^a Ref 17.

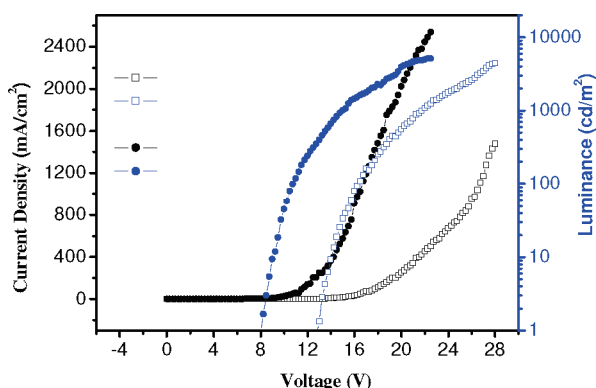


Figure 7. Current density-voltage-brightness characteristics of **PSiC8OF0** under two different devices. Open square for device a and filled circle for device b, black for current density and blue for luminance.

polymer film coated on a Pt electrode was performed in an electrolyte of 0.1 M tetrabutylammonium perchlorate in acetonitrile using ferrocene as the internal standard. In this work, the electrode potentials were recorded against the Ag/AgCl quasi-reference electrode. The potential of this reference electrode was calibrated using a ferrocene/ferrocenium redox

couple as an internal standard. The half-wave potential value of Fc was 0.55 eV. Therefore, the following two equations were used to calculate the energy levels of the $E_{\text{HOMO}} = -[E_{\text{onset}}^{\text{ox}} + 4.8 - 0.55]$ eV and $E_{\text{LUMO}} = -[E_{\text{onset}}^{\text{red}} + 4.8 - 0.55]$ eV.

Typical cyclic voltammograms of **PSiC8OFs** are shown in Figure 4 with related electrochemical data summarized in Table 4. The onset oxidation potentials are situated at 1.59–1.78 V and onset reduction potentials are situated at –1.24––1.46V for **PSiC8OFs**, from which their HOMO levels are estimated to be –5.84 to –6.07 eV, and their LUMO levels estimated to be –3.01 to –2.79 eV, respectively. The results show that the introduction of silyl units and jacketed units containing oxadiazole side groups decreased the LUMO level and facilitated electron injection. These results indicate that the introduction of electron-deficient moieties affect the electrochemical properties of the resulting polymers.

Electroluminescence Properties of LED Devices. To investigate the electrical properties and performances of the copolymers in real devices, two polymer EL devices with the configuration of (a) ITO/PEDOT:PSS[poly(ethylenedioxythiophene):polystyrenesulfonate]/polymer/TPBI[1,3,5-tris(*N*-phenylbenzimidazol-2-yl)benzene]/Ca(30nm)/Ag(80nm) and (b) ITO/PEDOT:PSS/PVK/polymer/TPBI (15nm)/Ca(30nm)/Ag(80nm) were fabricated. Figure 5 shows the EL spectra of **PSiC8OFs** under device a and EL spectra of **PSiC8OF0** under different voltages. The major emission peaks of the **PSiC8OFs** device are situated at 426 and 491nm, which are red-shifted compared to that in the PL spectra. As the **35C8** fraction increased, **PSiC8OF5** and **PSiC8OF10** exhibited emission at 426 nm which blue-shifted a lot and showed pure blue light, which maybe due to the big sterical jacketed units. However, as **35C8** content increased further, the color purity decreased. As can be seen in Figure 5(b), **PSiC8OF0** exhibited stable bright-blue EL emission band at 491 nm and the emission was independent of voltages. The EL emission of **PSiC8OF0**

changed little with variation of voltages. As the jacketed moiety increased, the EL emission of copolymers varied with voltages, which maybe attributed to the formation of "excimer-like" state. All of the copolymers show blue light, which may make them good blue light candidates for application in polymer LEDs.

Figure 6 shows the luminance and current efficiency versus bias characteristics of copolymers with the device **b**: ITO/PEDOT:PSS/PVK/polymer/TPBI (15 nm)/Ca (30 nm)/Ag (80 nm), and the related characteristic data are summarized in Table 5. Here, PVK was facilitate for hole injection and TPBI was used for hole blocking and electron transporting. The turn-on voltages (at 1 cd/m²) of the EL devices are in the range of 8.1 ~ 10.2 V. Specifically, the maximal current efficiency and external quantum efficiency of the **PSiC8OF5** device are 0.484 cd/A and 1.35%, respectively, and the maximum brightness of the **PSiC8OF0** device is 5105.4 cd/m², which surpasses those of the **PC8OF0** device (0.416 cd/A, 0.51% and 3122.8 cd/m²). The results suggest that the improvement in EL device performance with **PSiC8OF5** is assigned to the introduction of jacketed and silyl units which facilitate electron injection and suppressed the aggregation in the conjugated polymer chains. It can be seen from the LUMO levels of copolymers that **PSiC8OF5** has the highest LUMO level which will be easy for electron injection.

PSiC8OF0 show higher brightness but lower efficiency than **PSiC8OF5**, which may be due to its less balanced carrier and large drain current. However, as the jacketed segment increased further, the device efficiencies decreased sharply, which may be attributed to the big contribution of excimer-like state. Figure 7 represents the current density and brightness characteristics of two devices containing **PSiC8OF0** as a function of the applied voltage. Obviously, device **b** shows the higher current density and much lower turn-on voltage which was attributed to better hole injection, transportation and carrier recombination. These preliminary data show that with silyl units and a low content of jacketed units, the color purity and efficiency of polyfluorene could be improved.

Conclusions

In summary, a series of novel copolymers containing a jacketed moiety and silyl units were successfully synthesized through Suzuki polycondensation (SPC). The polymers exhibited high thermal stability with their glass transition temperatures in the range of 118~173 °C. The absorption and PL spectra of copolymers far blue-shifted compared to polyfluorene, originated from silyl and jacketed units. The transient PL spectra show an additional long decay time around 5~6 ns assigned to an "excimer-like" state, and its contribution increases with the increased jacketed fraction. Electrochemical results suggest that the incorporation of jacketed and silyl units decreased the LUMO level and facilitated electron injection. The maximal current efficiency and external quantum efficiency of the **PSiC8OF5** device are 0.484 cd/A and 1.35%, respectively, which surpass those of the **PC8OF0** device (0.416 cd/A and 0.51%), indicating that copolyfluorenes containing silyl units and a low content of the jacketed segment could be good candidates for blue light-emitting materials.

Acknowledgment. This work was supported by the National Natural Science Foundation of China (Nos. 20574002, 20634010, 90401028, and 50673003), and 973 program of People's Republic of China (No. 2002CB613405).

References and Notes

- (1) (a) Burroughes, J. H.; Bradley, D. D. C.; Brown, A. R.; Marks, R. N.; Mackay, K.; Friend, R. H.; Burn, P. L.; Holmes, A. B. *Nature (London)* **1990**, 347, 539. (b) Yang, Y.; Heeger, A. J. *Nature (London)* **1994**, 372, 344. (c) Friend, R. H.; Gymer, R. W.; Holmes, A. B.; Burroughes, J. H.; Marks, R. N.; Taliani, C.; Bradley, D. D. C.; dos Santos, D. A.; Bredas, J. L.; Logdlund, M.; Salaneck, W. R. *Nature (London)* **1999**, 397, 121. (d) Cao, Y.; Parker, I. D.; Yu, G.; Zhang, C.; Heeger, A. J. *Nature (London)* **1999**, 397, 414. (e) Jin, S. H.; Kim, M. Y.; Kim, J. Y.; Lee, K.; Gal, Y. S. *J. Am. Chem. Soc.* **2004**, 126, 2474.
- (2) (a) Zhang, X.; Shetty, A. S.; Jenekhe, S. A. *Macromolecules* **1999**, 32, 7422. (b) Zhang, X.; Jenekhe, S. A. *Macromolecules* **2000**, 33, 2069. (c) Liao, L.; Pang, Y.; Ding, L.; Karasz, F. E. *Macromolecules* **2001**, 34, 7300. (d) Jenekhe, S. A.; Lu, L.; Alam, M. M. *Macromolecules* **2001**, 34, 7315.
- (3) (a) Zhang, X.; Kale, D. M.; Jenekhe, S. A. *Macromolecules* **2002**, 35, 382. (b) Zhu, Y.; Alam, M. M.; Jenekhe, S. A. *Macromolecules* **2002**, 35, 9844. (c) Zhu, Y.; Alam, M. M.; Jenekhe, S. A. *Macromolecules* **2003**, 36, 8958. (d) Yang, J.; Jiang, C.; Zhang, Y.; Yang, R.; Yang, W.; Hou, Q.; Cao, Y. *Macromolecules* **2004**, 37, 1211. (e) Lu, J.; Tao, Y.; D'orio, M.; Li, Y.; Ding, J.; Day, M. *Macromolecules* **2004**, 37, 2442. (f) Tonzola, C. J.; Alam, M. M.; Bean, B. A.; Jenekhe, S. A. *Macromolecules* **2004**, 37, 3554.
- (4) (a) Heeger, A. J. *Solid State Commun.* **1998**, 107, 673. (b) Sheats, J. R.; Antoniadis, H.; Hueschen, M.; Leonard, W.; Miller, J.; Moon, R.; Roitman, D.; Stocking, A. *Science* **1996**, 273, 884.
- (5) (a) Hancock, J. M.; Gifford, A. P.; Zhu, Y.; Lou, Y.; Jenekhe, S. A. *Chem. Mater.* **2006**, 18, 4924. (b) Zhu, Y.; Champion, R. D.; Jenekhe, S. A. *Macromolecules* **2006**, 39, 8712.
- (6) (a) Scherf, U.; List, E. J. W. *Adv. Mater.* **2002**, 14, 477. (b) Becker, S.; Ego, C.; Grimsdale, A. C.; List, E. J. W.; Marsitzky, D.; Pogantsch, A.; Setayesh, S.; Leising, G.; Müllen, K. *Synth. Met.* **2002**, 125, 73. (c) Babel, A.; Jenekhe, S. A. *Macromolecules* **2003**, 36, 7759. (d) Hsieh, B. Y.; Chen, Y. *Macromolecules* **2007**, 40, 8913.
- (7) (a) List, E. J. W.; Guentner, R.; Freitas, P. S. D.; Scherf, U. *Adv. Mater.* **2002**, 14, 374. (b) Zhao, W.; Cao, T.; White, J. M. *Adv. Funct. Mater.* **2004**, 14, 785. (c) Zhou, X. H.; Zhang, Y.; Xie, Y. Q.; Cao, Y.; Pei, J. *Macromolecules* **2006**, 39, 3830.
- (8) (a) Cheon, C. H.; Joo, S.-H.; Kim, K.; Jin, J.-I.; Shin, H.-W.; Kim, Y.-R. *Macromolecules* **2005**, 38, 6336. (b) Wu, C. W.; Lin, H. C. *Macromolecules* **2006**, 39, 7232. (c) Hung, M.-C.; Liao, J.-L.; Chen, S.-A.; Chen, S.-H.; Su, A.-C. *J. Am. Chem. Soc.* **2005**, 127, 14576.
- (9) Redecker, M.; Bradley, D. D. C.; Inbasekaran, M.; Woo, E. P. *Appl. Phys. Lett.* **1998**, 73, 1565.
- (10) (a) Kraft, A.; Grimsdale, A. C.; Holmes, A. B. *Angew. Chem., Int. Ed.* **1998**, 37, 402. (b) Kim, D. Y.; Cho, H. N.; Kim, C. Y. *Prog. Polym. Sci.* **2000**, 25, 1089. (c) Akcelrud, L. *Prog. Polym. Sci.* **2003**, 28, 875.
- (11) (a) Pei, Q.; Yang, Y. *Adv. Mater.* **1995**, 7, 559. (b) Nikos, P. T.; Joannidis, K. K. *J. Polym. Sci., Part A: Polym. Chem.* **2005**, 43, 1049.
- (12) (a) Kim, K. D.; Park, J. S.; Kim, H. K.; Lee, T. B.; No, K. T. *Macromolecules* **1998**, 31, 7267. (b) Li, H.; West, R. *Macromolecules* **1998**, 31, 2866. (c) Miller, R. D.; Michl, J. *Chem. Rev.* **1989**, 90, 1359.
- (13) (a) Chen, Z.-K.; Huang, W.; Wang, L.-H.; Kang, E.-T.; Chen, B. J.; Lee, C. S.; Lee, S. T. *Macromolecules* **2000**, 33, 9015–9025. (b) Corey, J. Y. "History Overview and Comparison of Silicon with Carbon" In *The Chemistry of Organic Silicon Compounds Part I*; Patai, S., Rappoport, Z., Eds.; John Wiley and Sons Ltd.: New York, 1989; Chapter 1, pp 1–56.
- (14) Ahn, T.; Song, S. Y.; Shim, H. K. *Macromolecules* **2000**, 33, 6764.
- (15) Zhou, Q. F.; Li, H. M.; Feng, X. D. *Macromolecules* **1987**, 20, 233.
- (16) Zhang, G. L.; Liu, Z. H.; Guo, H. Q.; Chuai, Y. T.; Zou, D. C. *Chem. J. Chin. Univ.* **2004**, 3, 397.
- (17) Wang, P.; Jin, H.; Yang, Q.; Liu, W. L.; Shen, Z. H.; Chen, X. F.; Fan, X. H.; Zou, D. C.; Zhou, Q. F., submitted.
- (18) Luliński, S.; Serwatowski, J. *J. Org. Chem.* **2003**, 68, 5384.
- (19) Ahn, T.; Jang, M. S.; Shim, H. K.; Hwang, D. H.; Zyung, T. *Macromolecules* **1999**, 32, 3279.
- (20) Maus, M.; Mitra, S.; Lor, M.; Hofkens, J.; Weil, T.; Herrmann, A.; Müllen, K.; De Schryver, F. C. *J. Phys. Chem. A* **2001**, 105, 3961.
- (21) Wang, B. B.; Zhang, X.; Jia, X. R.; Li, Z. C.; Ji, Y.; Yang, L.; Wei, Y. *J. Am. Chem. Soc.* **2004**, 126, 15180.

MA801619D